Acta Scientiarum. Technology
ISSN: 1806-2563
ISSN: 1807-8664
actatech@uem.br
Universidade Estadual de Maringá
Brasil

Numerical two-dimensional thermal analysis of the human skin using the multigrid method

Ströher, Gylles Ricardo; Santiago, Cosmo Damião
Numerical two-dimensional thermal analysis of the human skin using the multigrid method
Acta Scientiarum. Technology, vol. 42, 2020
Universidade Estadual de Maringá, Brasil
Available in: https://www.redalyc.org/articulo.oa?id=303265671002
DOI: https://doi.org/10.4025/actascitechnol.v42i1.40992

Biotechnology

Numerical two-dimensional thermal analysis of the human skin using the multigrid method

Gylles Ricardo Ströher
Universidade Tecnológica Federal do Paraná, Brasil
gylles@utfpr.edu.br

Cosmo Damião Santiago
Universidade Tecnológica Federal do Paraná, Brasil

DOI: https://doi.org/10.4025/actascitechnol.v42i1.40992
Redalyc: https://www.redalyc.org/articulo.oa?id=303265671002

Received: 14 December 2017
Accepted: 30 April 2019

Abstract:

Heat can be used as an adjuvant treatment of many diseases and also as a powerful tool to help diagnose cancers, with the advantage to be a noninvasive exam. Some tumors may be best diagnosed by evaluating body temperature distribution, for instance, it is observed that local temperatures of the skin over a tumor are higher than the average skin temperature. Certainly, it is expected from medical diagnostics to be, early, fast and very precise. Especially if the health problem is a tumor, it is necessary to know the shape and the size of the cancer. Thermal images can provide further information about the tumor, generally, the thermal diagnostic is made comparing images of the region with a bioheat model. In this context, the present study shows interesting results about the multigrid method applied to solve the Pennes bioheat equation in two dimensions, using a non-stationary and steady state cases for the skin heath and with melanoma. The multigrid method presented itself as an extremely efficient and fast tool to solve the bioheat equation with refined grids that provide good spatial precision.

Keywords: thermal analysis, human skin, melanoma, pennes model, multigrid.

Introduction

The use of heat for therapeutic purposes dates back to ancient times. Egyptians, Romans, Greeks and other ancient people used it to treat various types of diseases and muscle problems (Ströher & Ströher, 2014). Currently, heat is used as an adjuvant treatment, and even as the main treatment tool. Heat is used, for instance, as a passive therapy in the treatment of pain and as an adjuvant treatment, and sometimes complementary, for the treatment of tumors. Some studies have shown that heating of tumors facilitates radio and chemotherapy. Krawczyk et al. (2011) suggest that high temperatures destroy enzymes that hinder the action of drugs that attack the disease, indicating that heat properly combined with some drugs improve the efficacy of chemotherapy.

Lima, Lyra, Guimarães, Carvalho, and Silva (2006) mention that inoperable duodenal tumors can be irradiated with laser sources endoscopically. The heat from the laser increases local temperature in order to kill the cancer cells without, however, causing thermal damage to healthy surrounding region.

Still regarding the use of heat in medicine, it can be used to help diagnose cancers, usually with the advantage to be a noninvasive test; e.g. infrared (IR) imaging has been widely used since the late 1950s (Agnelli, Barrea, & Tuner, 2011). González (2011) states that the results of metabolic heat production of breast tumors using infrared digital images (digital infrared imaging) has the potential to noninvasively estimate the malignancy of a tumor. More recently Strąkowska, Strąkowski, Strzelecki, Mey, and Więcek (2018) presented a new Active Thermography (AT) based method for detection of skin pathologies. The method was tested on a group of patients with psoriasis, however the authors explain that AT can be extended for screening other pathologies of the skin and the inner tissues.

Lawson (1956) was one the first to observe that local temperatures of the skin over a tumor were significantly higher (about 2 or 3 degrees) than normal skin temperature. Lawson and Chughtai (1963) established that the local difference in temperature over an embedded tumor was due to convection effects associated with increased blood perfusion and the increased metabolism around the tumor.

Gavriloaia, Ghemigian, and Hurduc (2009) used a very sensitive sensor, composed by a video camera showing its spatial position and a special computer fusion program, which were used for early cancer diagnosis. By using high-resolution maps, the diagnosis for about 78.4% of patients with thyroid cancer, and more than 89.6% from patients with breast cancer, were correct.

Centigul and Herman (2010) compared data obtained by imaging benign and malignant pigmented lesions; they measured surface temperature distributions for characteristic time instants, as well as temperatures of selected points on the surface of healthy skin, and compared them as a function of time. The results showed a distinct difference in the thermal responses between healthy tissue and the malignant lesion, and the thermal response of benign lesions was found to be similar to that of healthy skin tissue. The authors concluded that this difference could be used to identify malignant lesions and quantify their malignant potential.

The differences in energy generation between the normal and the cancerous tissues may be expressed as a higher local temperature around 2 to 3oC on the skin surface above the tumor Gautherie (1990). These higher temperatures can be easily detected by an Infrared (IR) camera as an abnormal thermogram. However, the results have been contradictory and often controversial. In particular, frequent occurrences of false-positive results have prevented thermography from becoming a standard early detection method. Chen, Pederson, and Chato (1977) have studied the feasibility and limitations of determining interior information from surface temperature field. They have performed a two-dimensional numerical simulation to examine the sensitivity of thermography and they conclude that for a deep lesion, thermography does not provide sufficient sensitivity for detection.

Osman and Afify (1988) numerically simulated the three-dimensional temperature profiles in the breast using the finite element method. They have correlated the tumor metabolic heat generation rate with the time required for the doubling of the tumor volume as measured by Gautherie (1990). Based on the simulations results, the authors claimed that abnormal surface temperature variations may not have a direct relation to an underlying tumor.

More recently, Herman (2013) mentions that with improvements in measurement technology as well as image and data analysis, better outcomes than those reported in the past studies have become a reality. In the current state-of-the-art, the temperature increase can be detected by IR quantum well cameras with a thermal sensitivity of 0.02oC (Minkowycz, 2009).

The majority of studies about tumors diagnostic uses experimental temperature data from the region of interest and through thermal models, metabolic heat generation and the modification in the physical properties values of regions with tumors are estimated.

Among the thermal models, Pennes' model (Osman & Afify, 1988) stands out for being widely used in the field of hyperthermia modeling, mainly because of its mathematical simplicity and by its ability to predict the temperature. There is also a deep discussion about which model is most appropriate to assess heat transfer using the conduction mode. Among the discussions are the classical Fourier's law of driving and the law that modifies Fourier, also known as Non-Fourier. In studies by Maillet (2019), Kumar, Singh, Sharma, and Rai (2018), Ströher and Ströher (2014), Ahmadikia, Fazlali, and Moradi (2012) and Xu, Seffen, and Lu (2008) are presented various results comparing the two approaches for heat conduction. The main goal of this study is to show results of the use of the multigrid method (Brandt, 1997; Trottenberg, Oosterlee, & Schüller, 2001) using the classical Fourier's law, without attempting to resolve the issue of the models of heat conduction, considering it as a limiting approximation. Both models, classical Fourier and Non-Fourier

are subjected to a non physical description of certain phenomena, like the well-known infinite propagation speed and the temperature overshoot phenomenon (Taitel, 1972).

The motivation for the use of the multigrid technique originates naturally from biothermic systems, because, of course, it is desirable for a medical diagnostic by thermal imaging to be as most accurate and fast as possible. In the same way, the ideal is that the solution of a thermal model also presents accurate and fast results, which requires a highly refined grid, mainly for early diagnostics in the tumor region can have small dimensions and also a short computational processing time.

The design and optimization of procedures of therapeutic measures like laser surgery, cryotherapy and magnetic nanoparticle based hyperthermia and radio frequency ablation has been aided by advancements in the understanding of bioheat transfer (Sarkar, Haji-Sheikh, & Jain, 2015), however until the moment there is not any study of multigrid methods applied in bioheat models.

The multigrid method has become a frequent choice in recent years especially since it satisfies the extremely refined grid requirement (Santiago, Marchi, & Souza, 2015). The computational effort of the multigrid method grows approximately linearly with the size of the problem which mainly depends on the complexity of the equation set to solve and the size of the grid. The size of the grid is directly related to the number of grid points. Therefore, gives it a good feature of scalability to become a very fast technique for the solution of large systems of algebraic equations.

In this study, it is proposed the development of a numerical solution for the 2D Pennes' equation in refined grids, with lower CPU time, in order to provide a numerical tool able to provide solutions with high accuracy in the spatial distribution of temperature. As a result, this work may give guidelines for medical procedures that use heat as a form of treatment and for the detection of tumors. The high accuracy of the numerical solution of temperature on skin can also assist in the verification of the temperature increase in regions with small melanomas, allowing early diagnosis, i.e. when the cancerous region is too small. The CPU time in grids up to 1025x1025 points was compared with the time taken from the numerical solution using the geometric multigrid method with V-cycle, and without using the multigrid method. It is important to emphasize that the authors have not found another studies available in the literature with the multigrid method for this physical problem.

Material and methods

In 1948, Pennes conducted a series of experiments that measured temperatures in forearms of human volunteers and derived the equation of conservation of thermal energy, the well-known bioheat transfer equation or the traditional bio-heat transfer equation (Pennes, 1948). It is written as Equation 1:

$$\rho_t c_t \frac{\partial T}{\partial t} = -\nabla q + \varpi_b c_b (T_a - T) + q_{met} + q_{ext} \tag{1}$$

where: ρt and ct are the density and specific heat of skin tissue, respectively; q is the heat flux vector representing heatflow per unit of time and area; is the blood perfusion rate; ρb and cb are the density and specific heat of the blood, respectively; Ta and T are the blood and skin tissue temperatures, respectively; qext is the heat generated by other heat sources; and qmet is the metabolic heat generation in skin tissue which is usually very small compared to the external power deposition term qext. The term , accounts for the effects of blood perfusion, and may be the dominant form of energy removal when considering heating processes. It assumes that the blood enters the control volume at some arterial temperature Ta, and then comes to

equilibrium at the tissue temperature. Thus, the blood that leaves the control volume carries away the energy, and hence acts as an energy sink in hyperthermia treatment. In the model, Equation 1, the conduction term can be based on Fourier's law, according Equation 2:

$$q(\vec{r},t) = -k\nabla T((\vec{r},t) \tag{2}$$

where: k is the thermal conductivity, #T is the temperature gradient, is the position vector, and t is the time. By combining Equation 1 and 2, is written as Equation 3:

$$\rho_t c_t \frac{\partial T}{\partial t} = k\nabla^2 T + \varpi_b c_b (T_a - T) + q_{met} + q_{ext} \tag{3}$$

As mentioned above, Pennes equation is based on the classic Fourier's law for heating, which assumes that the propagation speed of any temperature disturbance or thermal wave is infinite. It's important to mention that the 2-D cartesian system can be an adequate simplification for 3-D hemispherical geometry as showed by Das and Mishra (2014), and as mentioned earlier, Equation 3 is based on the classic Fourier's law for heating, which assumes that the propagation speed of any temperature disturbance or thermal wave is infinite. In the present study the melanoma is modeled as a source term equal to the total metabolic heat production in the tumor, as may be observed in Equation 3.

Discretization of mathematical model

The computational domain, in the present case 2D (i.e., the region in which it is desired to simulate the temperature distribution in human skin, defined by), is partitioned into a number of nodes (or points), given by , where is the total number of points in the grid, are the number of points in each spatial direction and is the domain length in each direction. A generic point P is located on the grid as , in which and , and , hx and hy are the distances between two consecutive points of the grid in x and y directions, respectively. To obtain a numerical solution, the Equation 3 was discretized with the Differences Finite Method (DFM) (Tannehill, Anderson, & Pletcher, 1997) in uniform grid, with central difference scheme of second order in space and the implicit scheme of Crank-Nicholson on temporal derivative. With the numerical approximations, Equation 3 may be written as Equation 4:

$$\frac{T_P^{n+1} - T_P^n}{\Delta t} = \frac{\eta_1}{h^2} T_E^{n+1} + \frac{\eta_1}{h^2} T_W^{n+1} + \frac{\eta_1}{h^2} T_N^{n+1} + \frac{\eta_1}{h^2} T_S^{n+1} - \frac{4\eta_1}{h^2} T_P^{n+1} + \eta_2 (T_a - T_P^n) + \eta_3 \tag{4}$$

where: , and , represent time and , . The indices , are the neighbors closest to the point in the directions x and y of the grid. Rearranging the terms of Equation 4, and writing it in general form of discretized equation in terms of the coefficients, we have Equation 5:

$$a_p T_p^{n+1} + a_E T_E^{n+1} + a_W T_W^{n+1} + a_N T_N^{n+1} + a_S T_S^{n+1} = b_P \tag{5}$$

in which the coefficients are given by Equation 6:

$$a_E = a_W = a_N = a_S = -\frac{\eta_1 \Delta t}{h^2},\ a_P = 1 + \frac{4\eta_1 \Delta t}{h^2} \text{ and } b_p = T_P^n + \Delta t(n_2(T_a - T_P^n) + \eta_3) \tag{6}$$

In the contours points, the coefficients are given by Equation 7:

$$a_E = a_W = a_N = a_S = 0,\ a_P = 1 \text{ and } b_p = T_{cc} \tag{7}$$

where: is the value of T in each point of the contour. The coefficients given by Equation 6 form a system of linear equations with dimension in the format with five diagonals that are resolved to the points in the interior of the domain. The temperature on the contours is approximated as follows: on the left contour and , and on the right, superior and inferior contours, respectively; is the heat flux applied on the skin. The index P indicates the point over the contour and E, W, S and N indicate the surrounding points inside the domain.

Solving the algebraic system

In each time step, the system of algebraic equations was solved with the Gauss-Seidel solver associated with the geometric multigrid method with V-cycle and FAS scheme. The Gauss-Seidel method was adopted with initial estimate the temperature of the skin, which is 37ºC. It was also adopted the coarsening ratio of 2 (default value in literature), i.e. the amount of points within the domain in any grid which is double the amount on the immediately coarser grid. An external iteration is characterized by a complete V-cycle, and an inner iteration is a smoothing performed by Gauss-Seidel solver. In a typical V-cycle in a FAS scheme, the system of algebraic equations is solved, Equation 5, with the coefficients of the contour, Equation 7, with few iterations in the loop where the numerical solution is desired (finest grid). The residue, which is given by , and the current approximation is transferred to the nearest corser grid. In this grid, the transferred solution is updated with the residue and a new system of linear equations is solved for a new approach. This procedure is repeated until reaching the coarsest specified grid. On this grid, the correction is interpolated and used to approximate the solution in the subsequent finer grid (post-smoothing). The systems of equations are solved at all levels of the grid. To transfer information between the grids, it was adopted direct injection into the restriction and bi-linear interpolation in prolongation. Other operators of transfer can be found in the literature (Briggs, Henson, & McCormick, 2000), but the most commonly used are adopted in this study. For each time step, the iterative process was interrupted when the ratio between the l1-norm of the kth iteration and the l1-norm of the first iteration (k1) is lower than 10^{-4}.

Results and discussion

This section is divided into three parts, the first presents the performance of the multigrid method, and the second presents the results about the verification of the numerical solution method, and the last shows the results of simulations when a region of the skin presents a malign melanoma tumor embedded in the skin tissue.

Numerical solution verification

Several studies on heat transfer perform thermal analysis of the skin. However, most of them use an one-dimensional approach, as the study of Jiang, Ma, Li, and Zhang (2002), Shih, Yuan, Lin, and Kou (2007), and Okajima, Maruyama, Takeda, and Komiya (2009), and other few studies used a two-dimensional approach. With the goal of verifying the numerical solution methodology proposed in the present study, we have simulated the same conditions in Ahmadikia et al. (2012), and Ströher and Ströher (2014) for a one-dimensional case, and Ströher and Ströher conditions for a two-dimensional case.

For the one-dimensional case, skin surface was subjected to a constant heat flux of 5000 W m^{-2}, another boundary in the x direction was set the zero heat flux condition boundary. The boundary conditions for y spatial coordinate were appropriately defined in order to become the one-dimensional problem. The results were summarized in Figure 1, that presents the temperature profile on the skin surface, x = 0 m, as a function of heating time.

Figure 1 shows that the numerical results of this study agree satisfactorily with the data from Ströher and Ströher (2014) and Ahmadikia et al. (2012), indicating that approach of the numerical solution applied is proper.

In the simulated two-dimensional case, a circular region with a diameter of two centimeters was subjected to a high heat flux, 8.5 MWm^{-2}, for 30 s on the skin surface. This event aims to simulate a possible situation of heating and subsequent cooling. The results are shown in Figure 2, which presents the distribution of temperature for the instants 5, 10, 30 and 120 s; Figure 2(a1)-(a3) shows results of Ströher and Ströher (2014) and Figure 2(b1)-(b3) of this work. It is noticeable that the predicted temperature distribution satisfactorily agrees with the distribution obtained by Ströher and Ströher (2014). It is observed in the instants shown that temperature distribution is almost flat during the initial instants and subsequently the temperature around the center of the heating point move away from the center, forming, in the figure of the scheme set up, a thermal cone.

Multigrid method perfomance

Simulations were performed to verify the performance of the multigrid method in relation to CPU time, but only the relevant results are shown in this paper. The algorithm with the FAS scheme was implemented in FORTRAN 2013, using the compiler Visual Studio 2010. The simulations were performed on a computer with an Intel Core I7 2.8 GHz processor with 4 GB of RAM, double precision.

Figure 3 shows the multigrid method performance for two-dimensional Pennes equations in transient and steady states. Figure 3(a) presents the results for the time-dependent problem, which simulates the temperature distribution on the skin with an external heat source at the center of the computational domain. For this case was adopted a physical time of 500 s, and tolerance of 10^{-4} over external iterations. The physical time was also used as a criterion for convergence in time.

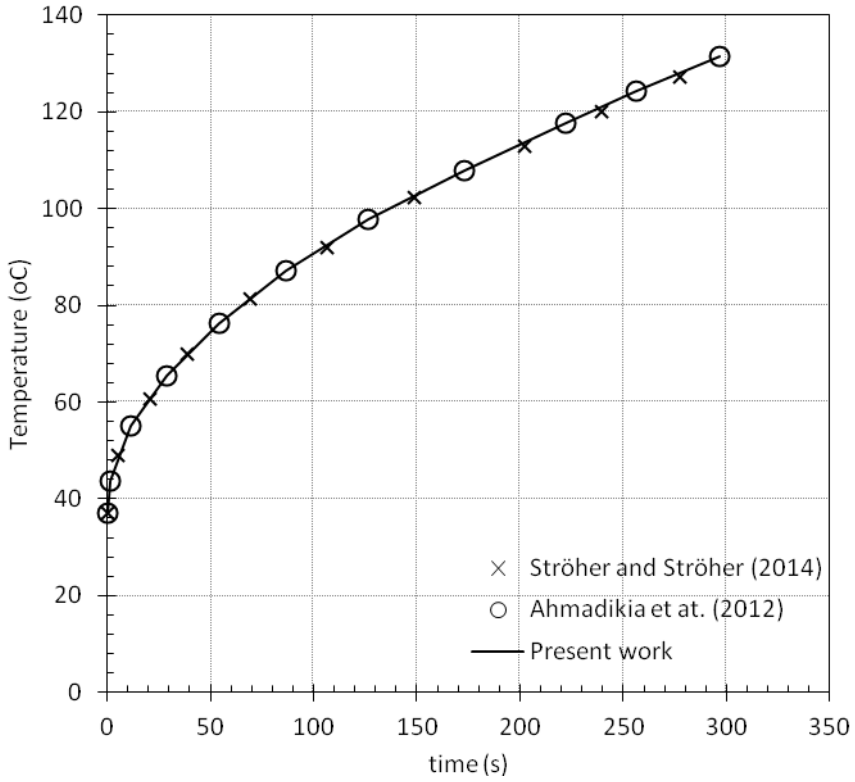

FIGURE 1
Skin surface temperature under constant heating boundary condition.

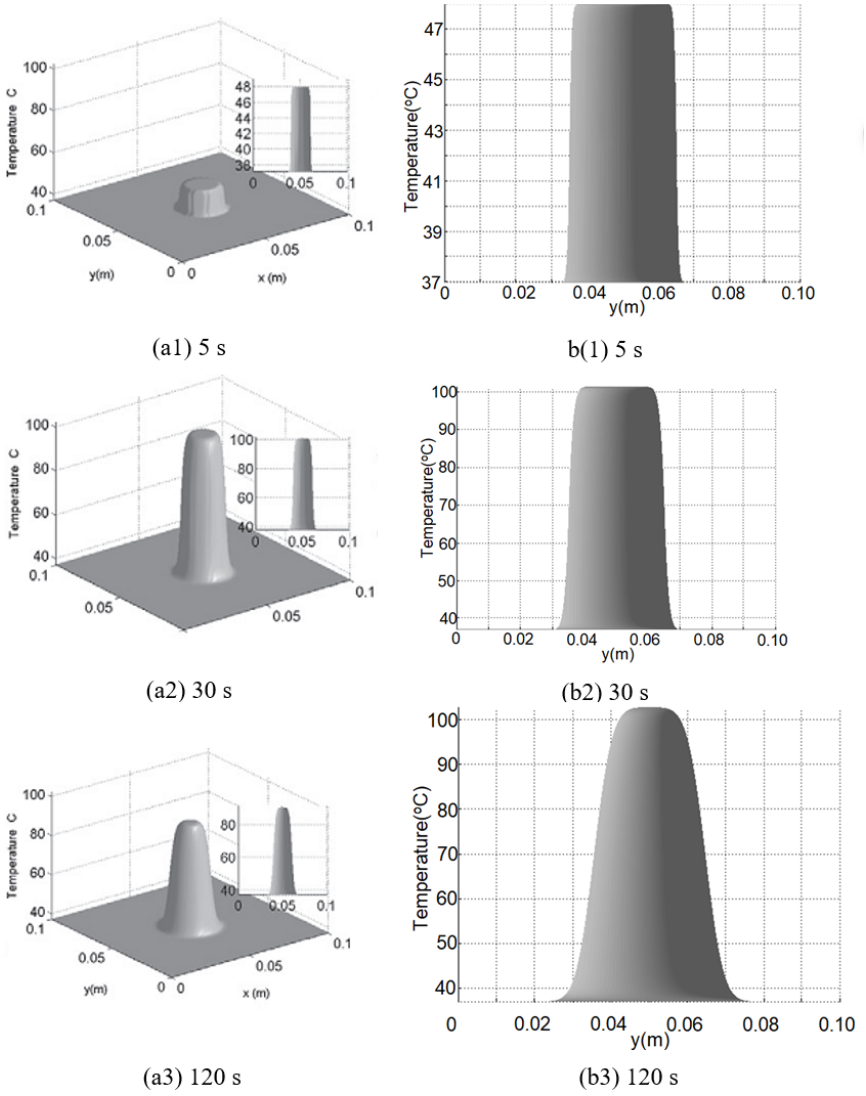

FIGURE 2.
Temperature distribution for the two-dimensional case: (a1)-(a3) Ströher and Ströher (2014); (b1)-(b3) present work.

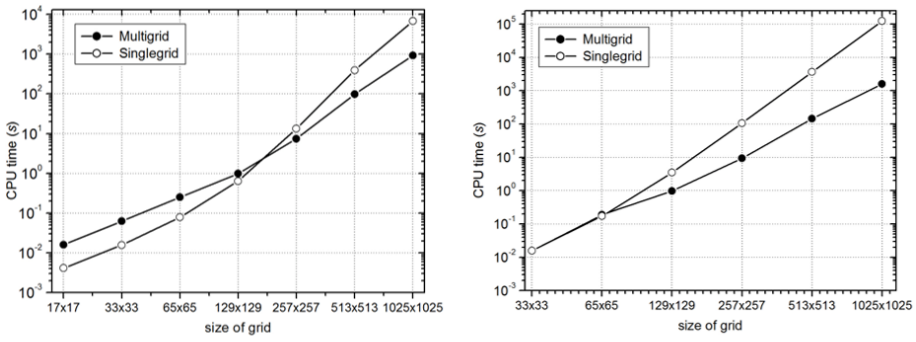

FIGURE 3.
Analysis of the performance of the multigrid method, with refining of grid in transient and steady states, of heat conduction in human skin with melanoma (a) transient; (b) steady state.

It is noted that the multigrid method has advantage over the singlegrid one only from the 129x129 points grid. For the 513x513 grid, the multigrid method is four times faster than the; for the grid 1025x1025 this ratio is 7.5 times faster. When the grid is refined in 4 times, the increase in CPU time is 9 times higher, on average. Although it is noticed an increased advantage of the multigrid method, this result is negligible when compared with the performance of multigrid methods for Poisson equation on a stationary state, a classic of literature. However, this weak performance may be attributed to the presence of the time derivative in Equation 3, as well as the physical characteristics of the model, as observed by (Santiago et al., 2015) for the Navier-Stokes equations in steady state. In each time step, the multigrid method algorithm runs using the Gauss-Seidel method, with two inner iterations until convergence. For example, for the grid 257x257, 125 steps in time are necessary. In each step, the multigrid makes four cycles V, i.e. check convergence in finest grid four times. This means that multigrid methods makes 500 convergence checks until it reaches the physical time established.

On the other hand, each iteration of the singlegrid method is cheaper than a V-cycle multigrid, but more iterations are needed for convergence. In this case, the solver was visited 2391 times, with 19 iterations on average in each step of time.

Figure 3(b) shows the results for the equation of Pennes in stationary state. Through the temperature difference, the model used in this study simulates a non-invasive diagnosis of a tumor on human skin. The performance of the multigrid was also influenced by physical parameters of this model. The multigrid method with the Gauss-Seidel solver was shown to be very sensitive in coarse grids, both in singlegrid and multigrid methods. In grids of less than 9 points, the solver diverged. Some tests were conducted with the SOR method with a too small under-relaxation factor, but the multigrid also proved unstable in some cases. Thus, the simulations with the Gauss-Seidel solver, using only an inner iteration, were performed with the multigrid method covering all the grids, where the coarsest grid used was 9x9 points. The best performance of the multigrid method is obtained with the maximum number of levels of grids, therefore, do not visit the coarsest grid can influence the multigrid performance. Figure 3(b) shows that the performance of the multigrid method was still significantly better than the shown in Figure 3(a), agreeing with the literature results (Santiago et al., 2015). This performance may be related to the absence of temporal derivative. In comparison with the singlegrid method, multigrid method presents advantages from 65x65 grid points. A linear increase in CPU time with N is also evident from these grids. In the grid 513x513, the multigrid method is 25 times faster than the singlegrid and the 1025x1025 grid surpasses it 77 times.

Melanoma simulation

Malignant melanoma is characterized by the uncontrolled growth of melanocytes, which are at the base of the epidermis, leading to irregular tumor shapes (Luna, Guerrero, Méndez, & Ortiz, 2014). The area of the skin attacked by a melanoma usually has different thermal properties of healthy skin. It may be highlighted that the metabolic generation rate is significantly higher in the tumor region, which naturally raises the temperature in the non-healthy region. Table 1 summarizes all physical properties used in this stage; the table shows the average thermal properties for healthy skin and for melanoma.

In order to observe the increase in temperature of skin with melanoma, we simulated a square region, 10x10 cm, with a circular 3 cm diameter melanoma at the center of the skin. Although melanomas normally do not present regular geometries, the motivation in this stage is to observe the influence of changes of the thermal properties on the distribution of skin temperature.

Since the multigrid method enables solutions with high spatial precision, we intended to evaluate how the thermal conduction process raises the temperature of healthy skin in the area near to the melanoma. In this case, a mesh 1025x1025 were used, i.e., Dx = Dy = 97.656 μm, resulting in about 308 nodal points in

the centerline of the melanoma, for example. Figure 4 and 5 show the numerical results obtained from the data of Table 1.

In Figure 4 the temperature contours for healthy skin and skin melanoma are shown; the temperature axis was intentionally set to intervals of 0.1°C since this corresponds to thermal sensitivity of most temperature measuring instruments, for example in case of thermal cameras. Figure 5 presents the temperature profiles for both cases; however in Figure 5(b) the temperature was scaled, $T^*(\%) = 100^*(T_{melanoma} - T_{healthy})/T_{healthy}$.

TABLE1
Values of the thermal properties used in the present work.

Tissue	q_{met} (W m^{-3})	k (W m^{-1} $^oC^{-1}$)	r (kg m^{-3})	w_b (ml s^{-1} ml^{-1})
Melanoma	6016[c]	0.558[a]	1050[a]	0.00085[b]
Skin	368.1	0.53[c]	1030[c]	0.0026[c]

a Cetingul and Herman (2010), b Vaupel, Kallinowsk, and Okunieff (1989), c Luna et al. (2014).

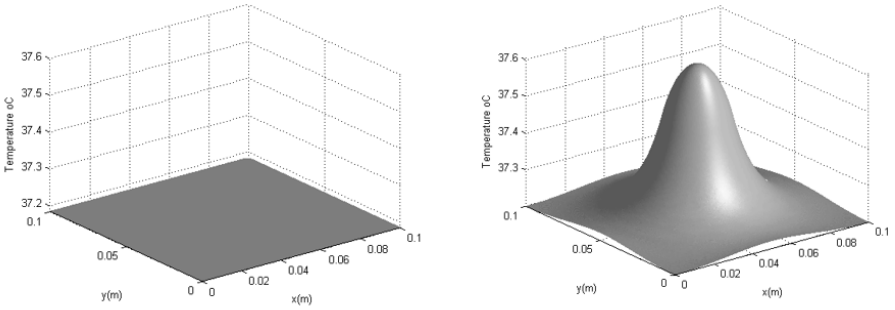

(a) (b)

FIGURE 4.
Temperature contour for (a) healthy skin, (b) skin with melanoma.

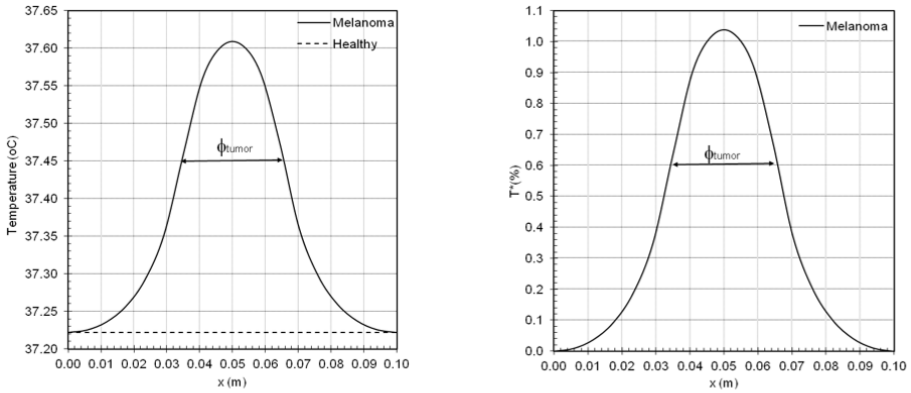

(a) (b)

FIGURE 5.
Temperature profile for healthy skin and skin with melanoma, f = diameter.
(a) Increase of Temperature and (b) Increase of Dimensionless Temperature.

Figure 5 shows that for simulated conditions the temperature increase due to the presence of melanoma is relatively small. The average temperature of healthy skin in thermal equilibrium is about 37°C, while for skin with the tumor, the temperature raises reaching the maximum value of 38.2°C. It is observed in Figure

5(b) that the maximum increase in temperature was about only 3%, which indicates the need of a thermal mapping equipment with high sensitivity for the determination or diagnostic of the tumor region. This result, corroborate with the work of Iljaž, Wrobel, Hriberšek, and Marn (2019) who argue that inverse problem analysis can be done only for exact date or low level of noise and advanced tumor. The temperature difference between the healthy tissue and early stage under steady-state conditions is very small, and the measurement error overrides this difference making the estimation of parameters very hard, even when fixing the metabolic heat generation and diameter of the tumor.

In order to observe the increase in temperature, we simulated many melanomas with different shapes and sizes. The simulated shapes presented round, square, rectangular and ellipsoid geometry. To perform a comparison between the results we used the area of the melanoma and a characteristic dimensionless length which was defined as Lc = 4*(Area/Perimeter)melanoma. The ratio area/perimeter was multiplied by 4 only to allow Lc to be equal to the diameter value for melanomas with round shape. The results are summarized in Figure 6 where are presented the maximum temperature reached versus the area and characteristic length.

It can observed from figure 6 that the increase in temperature is generally small; certainly the maximum temperature increases with Lc, since the area with the physical properties and metabolic heat generation affected by the tumor are also larger. the maximum temperature of the skin obtained with round, rectangular and square melanomas were slightly different, while for the ellipse shape the maximum temperature is significantly higher. in Figure 6(b) is observed that for small damaged areas the higher temperatures obtained are similar, independently of the shape of the melanoma. for the ellipsoid-shaped cases, it is possible to notice an increase in the maximum temperature in the injured region, more than for other geometries explored.

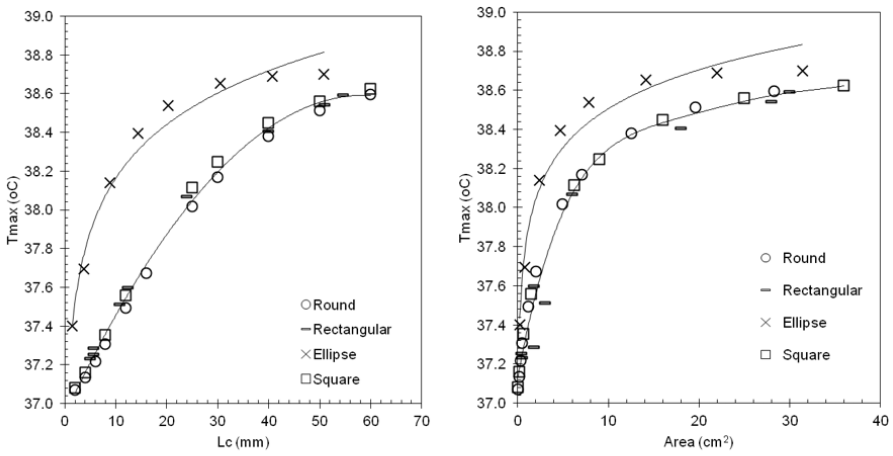

FIGURE 6.
Melanoma's maximum temperature associated with (a) caracheristc length and (b) area.

The maximum temperatures obtained in the present study corroborated the results of Hu, Gupta, Gore, and Xu (2004), where a breast cancer was simulated using the finite volume method using the software Fluent with a metabolic rate of 29 kW m^{-3} in the tumor region. Hu et al. (2004) present results of temperature increase for tumors located at a depth of 2 and 5 cm from the surface of the breast, with a temperature increase of 0.09 to 1.72 °C.

In general, the results presented in this study suggest that the diagnosis of melanoma type tumors must be carried out with a high thermal sensitivity in order to avoid any false positives. In the current state-of-the-art, the increase in temperature can be detected by IR quantum well cameras with a thermal sensitivity of 0.02°C. In a recent study, Herman (2013), using the Quaint (Quantification Analysis of Induced Thermography) imager, obtained an increase of temperature in 37 patients and the lesions were scanned prior to the biopsy.

Three of the 37 lesions were cancerous (determined by biopsy) and all three were successfully detected using Quaint. There were no false positives or false negatives detected using dynamic IR imaging tool. The temperature difference measured for a 2 mm diameter melanoma lesion was around 0.3°C.

Conclusion

For the case of the non-steady state model, there is an accentuated decrease in the speed-up of the multigrid method over the singlegrid. For the steady state model, the multigrid method provided a slight acceleration over singlegrid, although the speed-up is still lower than expected. The numerical results simulated for a typical melanoma indicated, for the simulated conditions, that the thermal mapping equipment should present high temperature sensitivity in order to determine accurately the boundaries of the melanoma.

Acknowledgements

The authors are very thankful to UTFPR for the financial support

References

Agnelli, J. P., Barrea, A. A., & Turner, C. V. (2011). Tumor location and parameter estimation by thermography. *Mathematical and Computer Modelling, 53*(7-8), 1527-1534. doi: 10.1016/j.mcm.2010.04.003

Ahmadikia, H., Fazlali, R., & Moradi, A. (2012). Analytical solution of the parabolic and hyperbolic heat transfer equations with constant and transient heatflux conditions on skin tissue. *International Communications in Heat and Mass Transfer, 39*(1), 121-130. doi: 10.1016/j.icheatmasstransfer.2011.09.016

Brandt, A. (1977). Multi-level adaptive solutions to boundary-value problems. *Mathematics of Computation, 31*(138), 333-390. doi: 10.2307/2006422

Briggs, W. L., Henson, V. E., & McCormick, S. F. (2000). *A multigrid tutorial* (2nd ed.). Philadelphia, PA: Siam. doi:10.1137/1.9780898719505.

Cetingul, M. P., & Herman, C. (2010). A heat transfer model of skin tissue for the detection of lesions: sensitive analysis. *Physics in Medicine and Biology, 55*(19), 59335951. doi: 10.1088/0031-9155/55/19/020

Chen, M. M., Pederson, C. O., & Chato, J. C. (1977). On the feasibility of obtaining three dimensional information from thermographic measurement. *Journal of Biomechanical Engineering, 99*(2), 58-64. doi: 10.1115/1.3426274

Das K, Mishra SC. (2014). Non-invasive estimation of size and location of a tumor in a human breast using a curve fitting technique. *International Communications in Heat and Mass Transfer,,* 56, 63-70. doi: 10.1016/j.icheatmasstransfer.2014.04.015

Gautherie, M. (1990). *Biological basis of oncologic thermoterapy*. Berlin, DE: Springer.

Gavriloaia, G., Ghemigian, A. M., Hurduc, A. E. (2009). Early cancer diagnosis by image processing sensors measuring the conductive or radiative heat. In C.T., Lim, & J. C. H., Goh (eds.), *13th International Conference on Biomedical Engineering* (Vol. 23). Berlin, Heidelberg: Springer,

González, F. J. (2011). Non-invasive estimation of the metabolic heat production of breast tumors using digital infrared imaging. *Quantitative InfraRed Thermography Journal, 8*, 139–148. doi:10.3166/qirt.8.139-148.

Herman, C. (2013). The role of dynamic infrared imaging in melanoma diagnosis. *Expert Rev Dermatol, 8*(2), 177-184. doi: 10.1586/edm.13.15

Hu, L., Gupta, A., Gore, J. P., & Xu, L. X. (2004). Effect of forced convection on the skin thermal expression of breast cancer. *Journal of Biomechanical Engineering, 126*(2), 204-211. doi: 10.1115/1.1688779

Iljaž, J., Wrobel, L. C., Hriberšek, M., & Marn, J. (2019). The use of design of experiments for steady-state and transient inverse melanoma detection problems. *International Journal of Thermal Sciences, 135*, 256-275. doi: 10.1016/j.ijthermalsci.2018.09.003

Jiang, S. C., Ma, N., Li, H. J., & Zhang, X. X. (2002). Effects of thermal properties and geometrical dimensions on skin burn injuries. *Burns, 28*(8), 713-717. doi: 10.1016/S0305-4179(02)00104-3

Krawczyk, P. M., Eppink, B., Essers, J., Stap, J., Rodermond, H., Odijk, H., Aten, J. A. (2011). Mild hyperthermia inhibits homologous recombination,induces BRCA2 degradation, and sensitizes cancer cells to poly (ADP-ribose) polymerase-1 inhibition. *Proceedings of the National Academy of Sciences, 108*(24), 9851-9856. doi: 10.1073/pnas.1101053108

Kumar, D., Singh, S., Sharma, N., & Rai, K. N. (2018). Verified non-linear DPL model with experimental data for analyzing heat transfer in tissue during thermal therapy. *International Journal of Thermal Sciences, 133*, 320-329. doi: 10.1016/j.ijthermalsci.2018.07.031

Lawson, R. N. (1956). Implications of surface temperatures in the diagnosis of breast cancer. *Canadian Medical Asociation Journal, 75*(4), 309-310.

Lawson, R. N., & Chughtai, M. S. (1963). Breast cancer and body temperatures. *Canadian Medical Asociation Journal, 88*(2), 68-70.

Lima, R. C. F., Lyra, P. R. M., Guimarães, C. S. C., Carvalho, D. K. E., & Silva, G. M. L. L. (2006). Modelagem da biotransferência de calor no tratamento por hipertermia de tumores pelo MVF. *Revista Brasileira de Engenharia Biomédica, 22*(2), 119-129.

Luna, J. M., Guerrero, A. H., Méndez, R. R., & Ortiz, J. L. L. (2014). Solution of the inverse bioheat transfer problemfor a simplified dermatological application: case of skin cancer. *Ingeniería Mecánica, Tecnología y Desarrollo, 4*(6), 219-228.

Maillet, D. (2019). A review of the models using the Cattaneo and Vernotte hyperbolic heat equation and their experimental validation. *International Journal of Thermal Sciences, 139*, 424-432. doi: 10.1016/j.ijthermalsci.2019.02.021

Minkowycz, W. J. (2009). *Advances in numerical heat transfer* (Vol. 3). Boca Raton, FL: CRC Press. doi: 10.1201/9781420095227

Okajima, J., Maruyama, S., Takeda, H., & Komiya, A. (2009). Dimensionless solutions and general characteristics of bioheat transfer during thermal therapy. *Journal of Thermal Biology, 34*(8), 377-384. doi: 10.1016/j.jtherbio.2009.08.001

Osman, M. M., & Afify, E. M. (1988). Thermal modelling of the malignant woman's breast. *ASME Journal of Biomechanical Engineering, 110*(4) 269-276. doi: 10.1115/1.3108441

Pennes, H. (1948). Analysis of tissue and arterial blood temperature in the resting human forearm. *Journal of Applied Physiology, 1*(2), 93-122. doi: 10.1152/jappl.1948.1.2.93

Santiago, C. D., Marchi, C. H., & Souza, L. F. (2015). Performance of geometric multigrid method for coupled two-dimensional systems in CFD. *Applied Mathematical Modelling, 39*(9), 2602-2616. doi: 10.1016/j.apm.2014.10.067

Sarkar, D., Haji-Sheikh, A., & Jain, A. (2015). Temperature distribution in multi-layer skin tissue in presence of a tumor. *International Journal of Heat and Mass Transfer, 91*, 602-610. doi: 10.1016/j.ijheatmasstransfer.2015.07.089

Shih, T.-C., Yuan, P., Lin, W.-L., & Kou, H.-S. (2007). Analytical analysis of the Pennes bioheat transfer equation with sinusoidal heat flux condition on skin surface. *Medical Engineering & Physics, 29*(9), 946-953. doi: 10.1016/j.medengphy.2006.10.008

Strąkowska, M., Strąkowski, R., Strzelecki, M., Mey, G., & Więcek, B. (2018). Thermal modelling and screening method for skin pathologies using active thermography. *Biocybernetics and Biomedical Engineering, 38*(3), 602-610. doi: 10.1016/j.bbe.2018.03.009

Ströher, G. R., & Ströher, G. L. (2014). Numerical thermal analysis of skin tissue using parabolic and hyperbolic approaches. *International Communications in Heat and Mass Transfer, 57*, 193-199. doi: 10.1016/j.icheatmasstransfer.2014.07.026

Taitel, Y. (1972). On the parabolic, hyperbolic and discrete formulation of the heat conduction equation. *International Journal of Heat and Mass Transfer, 15*(2), 369-371. doi: 10.1016/0017-9310(72)90085-3

Tannehill, J. C., Anderson, D. A., & Pletcher, R. H. (1997). *Computational fluid mechanics and heat transfer* (2nd ed.). Philadelphia, PA: Taylor & Francis.

Trottenberg, U., Oosterlee, C. W., & Schüller, A. (2001). *Multigrid*. New York: Academics Press.

Vaupel, P., Kallinowsk, F., & Okunieff, P. (1989). Blood flow, oxygen, nutrient supply and metabolic microenvironment of human tumors: a review. *Cancer Research, 49*(23), 64496465.

Xu, F., Seffen, K. A., & Lu, T. J. (2008). Non-Fourier analysis of skin biothermomechanics. *International Journal of Heat and Mass Transfer, 51*(9-10), 2237-2259. doi: 10.1016/j.ijheatmasstransfer.2007.10.024